

Image Denoising Using M-Band Wavelets

A Study on M-Band Wavelet and its Application for Image Denoising

Kaushik Sinha

Assistant Professor, Dept. of IT
College of Engineering and Management, Kolaghat
KTPP Township, West Bengal, India

Debalina Jana

Assistant Professor, Dept. of AEIE
College of Engineering and Management, Kolaghat
KTPP Township, West Bengal, India

Abstract—This work addresses to a study on the different techniques of noise removal from an image using M-Band Wavelet Transform. The standard wavelet transform technique has already proven its capability for different image processing problems such as image denoising. Noise removal from image is best done in the frequency domain. Psychophysical results indicate human visual processes an image by decomposing into multiple channels corresponding to its frequency and orientation components at different scales. It is also capable of preserving both local and global information. So, multi scale wavelet analysis is an ideal approach to describe noise removal. In this paper, the capability of M-Band Wavelet Transform is discussed in the process of noise removal from different images.

Keywords—M-Band Wavelet Transform; Additive White Gaussian noise; Thresholding; Image Denoise

I. INTRODUCTION

Many types of noises due to sensor or channel transmission errors often corrupt images and noise suppression becomes a particularly delicate and a difficult task [5-6]. Applied noise removal techniques should take into account a trade-off between noise reduction and preservation of actual image content in a way that enhances the diagnostically relevant image content.

The need for efficient image restoration methods has grown with the massive production of digital images and movies of all kinds, often taken in poor conditions. No matter how good cameras are, an image improvement is always desirable to extend their range of action [4].

The two main limitations in image accuracy are categorized as blur and noise. Blur is intrinsic to image acquisition systems, as digital images have a finite number of samples and must satisfy the Shannon–Nyquist sampling conditions. The second main image perturbation is noise. There are different types of noises that can affect an image. Some of them are

A. Salt and pepper noise

It is the type of noise where some black and white pixels occurs randomly on an image. A false saturation gives a white spot (salt) and a failed response gives a black spot in the image (pepper) [3], [9].

B. Gaussian white noise

This is the most common type of noise [3], [7-9] which can be generated artificially using the formula

$$Y = X + \text{sqrt}(\text{variance}) \times \text{random}(s) + \text{mean}; \quad (1)$$

Where, X is the input image, Y is the output image, s is the size of X. The value of mean and variance is taken as input.

C. Poisson noise

In probability theory and statistics, Poisson distribution is a discrete probability distribution that expresses the probability of a number of events occurring in a fixed interval of time and/or space. If the expected number of occurrences in a particular time interval is λ , then probability that there are exactly k (k = 0, 1, 2 ...) occurrences is given by

$$f(k, \lambda) = \frac{\lambda^k e^{-\lambda}}{k!} \quad (2)$$

D. Speckle noise

Within each resolution cell, a number of elementary scatters reflect the incident wave towards the sensor. The received image is thus corrupted by a random granular pattern, called Speckle. A speckle noise can be modelled as

$$v = f\vartheta \quad (3)$$

Where, v is the speckle noise, f is the noise-free image and ϑ is a unit mean random field. In this paper, the experimental work is done with Gaussian white noise [9].

In the field of Image Processing, the wavelet transform has emerged with a great success [10]. The M-band wavelet transform[24] is a specific area of wavelet transform which has so many advantages over standard wavelet transform [17-23].

II. M-BAND WAVELET TRANSFORM

The term wavelet means a small wave. The smallness refers to the condition that this (window) function is of finite length (compactly supported). The wave refers to the

condition that this function is oscillatory [6]. The wavelet transform (WT) is a powerful tool of signal processing for its multiresolutional possibilities [2]. Unlike the Fourier transform, the WT is suitable for handling the non-stationary signals – variable frequency with respect to time.

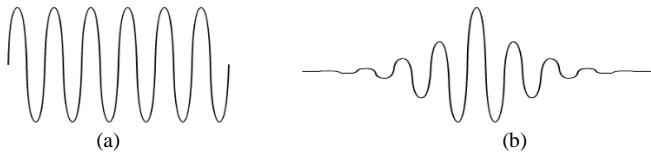


Fig. 1 Representation of a wave (a), and a wavelet (b)

The illustration in figure 2 is commonly used to explain how time and frequency resolutions should be interpreted. Every box in figure 2 corresponds to a value of the wavelet transform in the time frequency plane. Note that boxes have a certain non-zero area, which implies that the value of a particular point in the time-frequency plane cannot be known. All the points in the time-frequency plane that falls into a box are represented by one value of the WT.

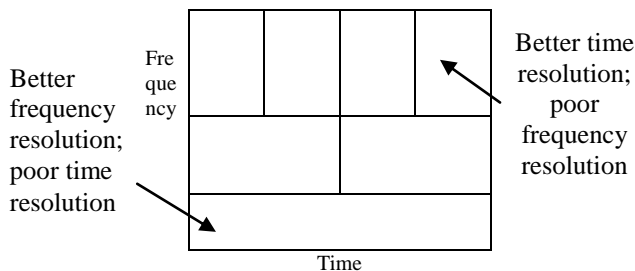


Fig. 2 Representation of time-frequency plane

First thing to notice in figure 2 is that although the widths and heights of the boxes change, the area is constant. That is each box represents an equal portion of the time-frequency plane, but giving different proportions to time and frequency. At higher frequencies the width of the boxes decreases, means the time resolution gets better, and the heights of the boxes increase, i.e., the frequency resolution gets poorer.

A. Discrete Wavelet Transform (DWT)

Consider an image $f(x,y)$ of size $M \times N$ whose forward discrete transform, $T(u, v, \dots)$ can be expressed in terms of the general relation [1]

$$T(u, v, \dots) = \sum_{x,y} f(x, y) g_{u,v,\dots}(x, y) \tag{4}$$

Where x and y are spatial variables and u, v, \dots are transform variables. Given $T(u, v, \dots)$, $f(x,y)$ can be obtained using generalized inverse discrete transform

$$f(x, y) = \sum_{u,v} T(u, v, \dots) h_{u,v,\dots}(x, y) \tag{5}$$

The $g_{u,v,\dots}$ and $h_{u,v,\dots}$ in these equations are called forward and inverse kernels respectively. They determine the nature computational complexity and ultimate usefulness of the transform pair.

The discrete wavelet transform (DWT) is a linear transformation that operates on a data vector whose length is an integer power of two, transforming it into a numerically different vector of the same length [1], [2].

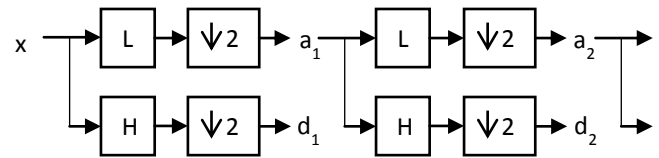


Fig. 3 DWT Tree

It separates data into different frequency components, and then matches each component with resolution to its scale. DWT is computed with a cascade of filters followed by a factor 2 subsampling.

H and L denotes high and low-pass filters respectively, $\downarrow 2$ denotes subsampling. Outputs of these filters are given by equations (6) and (7).

$$a_{j+1}[p] = \sum_{n=-\infty}^{+\infty} l[n - 2p] a_j(n) \tag{6}$$

$$d_{j+1}[p] = \sum_{n=-\infty}^{+\infty} h[n - 2p] a_j(n) \tag{7}$$

Elements a_j are used for next step (scale) of the transform and elements d_j , called wavelet coefficients, determine output of the transform. $l[n]$ and $h[n]$ are coefficients of low and high-pass filters respectively. Assume that on scale $j+1$ there is only half from number of a and d elements on scale j .

DWT algorithm for two-dimensional pictures is similar. The DWT is performed firstly for all image rows and then for all columns (figure 4) [20], [22].

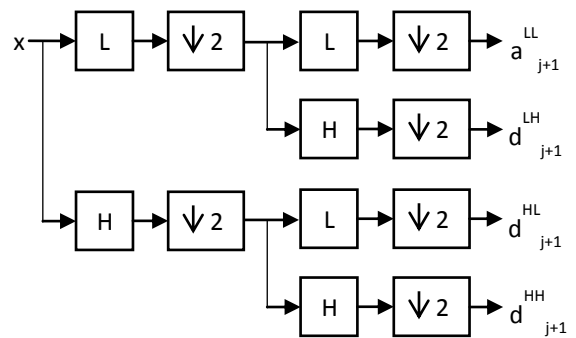


Fig. 4 Wavelet Decomposition for 2D Signals

A vector contains energies of wavelet coefficients calculated in sub-bands at successive scales. As a result of this transform there are 4 subband images [21], [23] at each scale (figure 5).

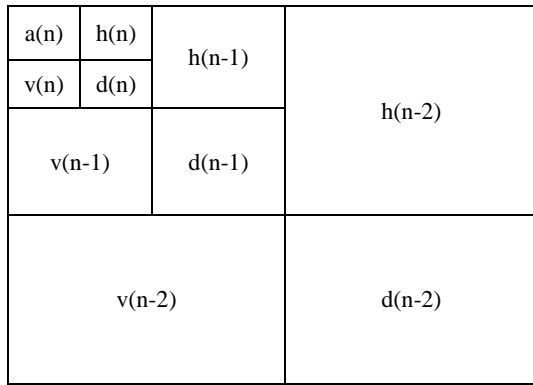


Fig. 5 Sub-band Images for Wavelet Decomposition

Sub band image ‘a’ is used only for DWT calculation at the next scale.

B. M-Band Wavelet Transform

The wavelet transform maps a function $f(x) \in L^2(\mathbb{R})$ onto a scale-space plane [18], [19]. The wavelets are obtained from a single prototype function $\psi(x)$ by scaling parameters a and shift parameters b. The continuous wavelet transform of a function $f(x)$ is given as,

$$Wf_a(b) = \int f(x)\psi_{a,b}^*(x)dx \tag{8}$$

M-band wavelet decomposition is a direct generalization of the above two-band case [25]. Let $\phi(x)$ be the scaling function satisfying,

$$\phi(x) = \sum_k h(k)\sqrt{M}\phi(Mx - k) \tag{9}$$

In addition there are M - 1 wavelets which also satisfy

$$\psi^{(j)}(x) = \sum_k \sqrt{M}h^{(j)}(k)\psi(Mx - k) \tag{10}$$

In discrete form these equations can be written as

$$\phi_{ik}(x) = \sum_k M^{-i/2}\phi(M^{-i}x - k) \tag{11}$$

$$\psi_{ik}^{(j)}(x) = \sum_k M^{-i/2}\psi^{(j)}(M^{-i}x - k) \tag{12}$$

A function $f(x) \in V^0 \in L^2(\mathbb{R})$ can be constructed from a discrete sequence $a(k) \in l^2(\mathbb{R})$ in the form,

$$f(x) = \sum_k a(k)\phi(x - k) \tag{13}$$

$f(x)$ can also be expressed in terms of the sum of projections onto subspaces V_i and $W_i^{(j)}$ as,

$$f(x) = \sum_k c(k)\phi_{i,k}(x) + \sum_{j=1}^{M-1} \sum_k d_j(k)\psi_{ik}^{(j)}(x) \tag{14}$$

The expansion coefficients can be expressed as,

$$c(k) = \langle f, \phi_{i,k} \rangle, \tag{15}$$

$$d_j(k) = \langle f, \psi_{i,k}^{(j)} \rangle, \quad j = 1, \dots, M - 1$$

Using (9) and (10) in (15), it can be shown that,

$$c(k) = \frac{1}{\sqrt{M}} \sum_l a(l)h(Mk - l) \tag{16}$$

$$d_j(k) = \sum_l a(l)h^{(j)}(Mk - l) \tag{17}$$

Which is equivalent to processing the sequence $a(k)$ with a set of linear time-invariant filters of impulse responses and down sampling filter outputs by M. The M-band wavelet system has been in the focus of several recent investigations [25]. Noteworthy advantages of M-band wavelet systems over two-band wavelet systems are their richer parameter space which leads to a greater variety of compactly supported wavelets. These are practically implementable and have their ability to achieve more rapidly a given frequency resolution as a function of decomposition scale. These facts provide greater freedom and flexibility in choosing time frequency tilling.

The structure of the classical one-dimensional filter bank problem [18] is given in figure 6. The filter bank problem involves the design of the real coefficient realizable. Closely related to the filter bank problem is the transmultiplexer problem. A transmultiplexer[18] is a device for converting time-domain-multiplexed (TDM) signals to frequency-domain-multiplexed signals (FDM).

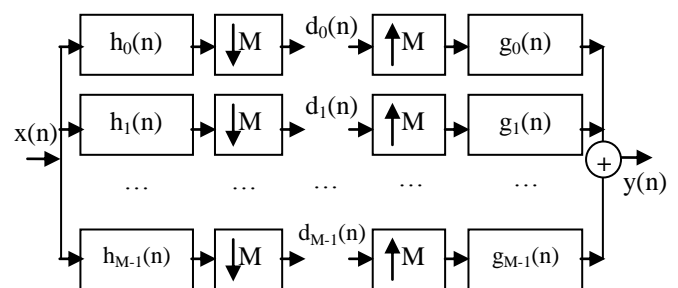


Fig. 6 An M-channel filter bank

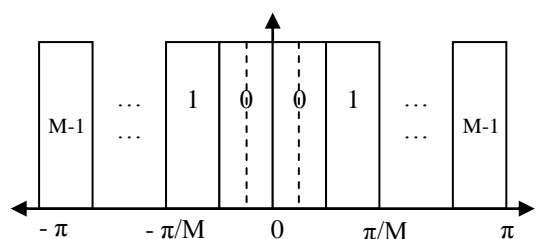


Fig. 7 Ideal frequency responses in an M-channel filter bank

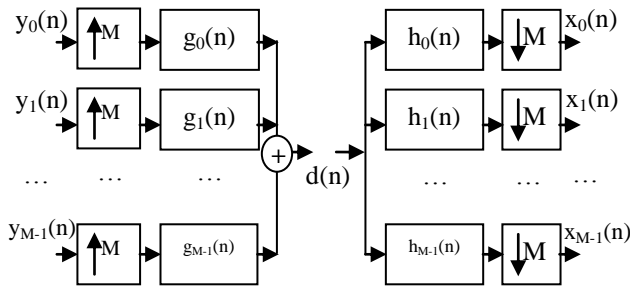


Fig. 8 An M-channel Trans-multiplexer

The basic structure of a transmultiplexer is shown in figure 8. The transmultiplexer problem is to design filters such that perfect reconstruction is guaranteed and the filter responses approximate in figure 7.

III. IMAGE DENOISING

Two main limitations in the image and noise model is given as equation (18)

$$X = S + \sigma \cdot g \tag{18}$$

Where, S is an original image and X is a noisy image corrupted by additive white Gaussian noise g of standard deviation σ . Both images s and X are of size N by M (mostly $M = N$ and always power of 2) [11-14].

A. Basic steps for image denoising

The basic steps involved in image denoising as followed in this paper is shown in the block diagram (figure 9) below.

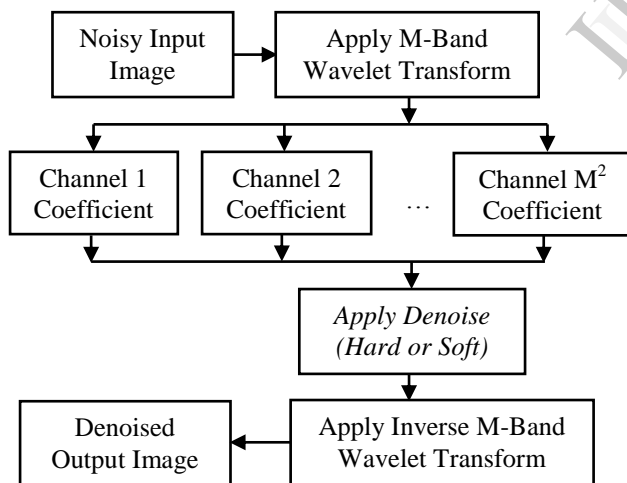


Fig. 9 Basic Steps for Image Denoising

B. Threshold Determination

The standard thresholding of wavelet coefficients is governed mainly by either 'hard' or 'soft' thresholding function [10] as shown in figure 10. The first function in figure 10(a) is a 'hard' function, and figure 2(b) is a 'soft' function [17].

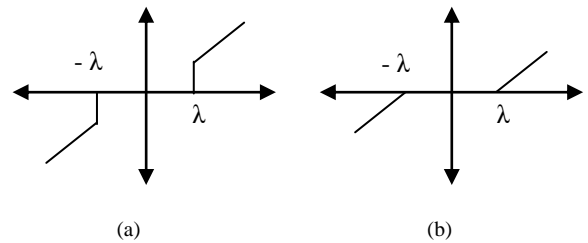


Fig. 10 Thresholding functions; (a) hard, (b) soft

The hard thresholding function is given as

$$z = \text{hard}(w) = \begin{cases} w, & \text{for } |w| > \lambda \\ 0, & \text{for } |w| \leq \lambda \end{cases} \tag{19}$$

Similarly, soft thresholding function is given as [14]

$$z = \text{soft}(w) = \begin{cases} \text{signum}(w) \times \max(|w| - \lambda, 0), & \text{for } |w| > \lambda \\ w, & \text{for } |w| \leq \lambda \end{cases} \tag{20}$$

Where, w and z are the input and output wavelet coefficients respectively, λ is a selected threshold value for both (19) and (20).

C. Performance Measurement

The performance of various denoising algorithms is quantitatively compared using MSE (mean square error) [5], [15] and PSNR [16] (Peak Signal to Noise Ratio) as

$$MSE = \frac{1}{NM} \sum_{n=1}^N \sum_{m=1}^M |s(n, m) - y(n, m)|^2 \tag{21}$$

$$PSNR = 10 \log_{10} \left(\frac{255^2}{MSE} \right) \tag{22}$$

Where, s is an original image and y(n,m) is a recovered image from a noisy image s(n,m).

IV. EXPERIMENTAL RESULTS AND DISCUSSION

The experiments are conducted (process was as shown in figure 9) taking M=4 (for M-Band) on natural greyscale test images like Lena, Barbara, Peppers, Boat etc. of size 512x512. The kind of noise, added to original image, is Gaussian of different noise levels $\sigma = 2, 5$ and 10 one after another. Figure 11 shows the original and noisy version of barbara image.

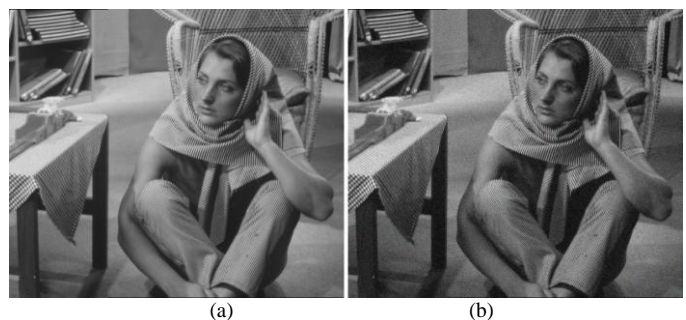


Fig. 11 Experimental Image of barbara (256x256) (a) Original, (b) After adding Gaussian White Noise of $\sigma=2$, variance=30

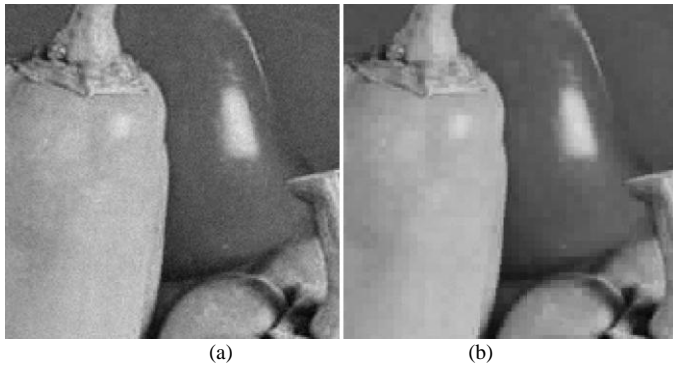


Fig. 12Peppers image 300% magnified; (a) Noisy, (b) Denoised Image

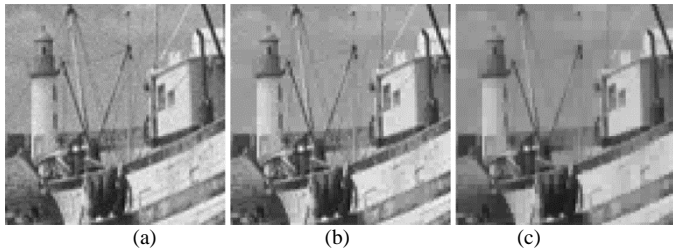


Fig. 13Boat Image 400% magnified (a)noisy image, (b)denoised image using hard threshold, (c) denoised image using soft threshold

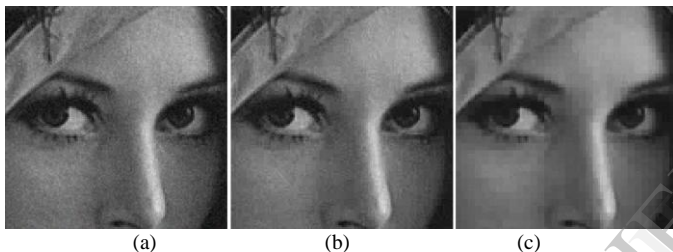


Fig. 14Lena Image 400% magnified (a)noisy image, (b)denoised image using hard threshold, (c) denoised image using soft threshold

The PSNR values as given in equation (21) and (22), are obtained as shown in table I. The PSNR from various methods are compared in Table I and the data are collected from an average of fifteen to twenty runs on the each image of size 512×512.

TABLE I
PSNR VALUES FOR IMAGES OF SIZE 512×512

Image Name	Th. Type ^a	Value of Sigma (σ)		
		2	5	10
lena	Hard	35.0385	30.5835	28.8199
	Soft	31.3728	27.3253	23.6765
barbara	hard	35.3577	30.0593	27.0913
	soft	30.9910	26.3386	22.7523
baboon	hard	36.0850	28.2366	24.1164
	soft	29.6279	24.1578	20.7253
boat	hard	35.1460	29.8883	27.4503
	soft	30.8520	26.4326	22.8586
fruits	hard	35.1648	30.0153	27.8897
	soft	31.0728	26.7965	23.3131
goldhill	hard	35.0529	29.5271	27.6074
	soft	30.7525	26.5456	23.1724
peppers	hard	35.1891	31.4086	29.5094
	soft	31.8152	27.6794	23.7337

^a. Type of threshold – hard or soft

From the PSNR values shown in table I, it is very much clear that, as we increase the value of noise level (σ), PSNR

value gradually decreases. A comparison among all the pictures are given in the following figure 15 and 16.

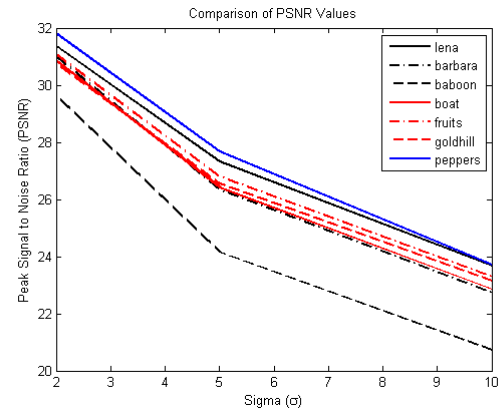


Fig. 15Comparison among all the images as graph

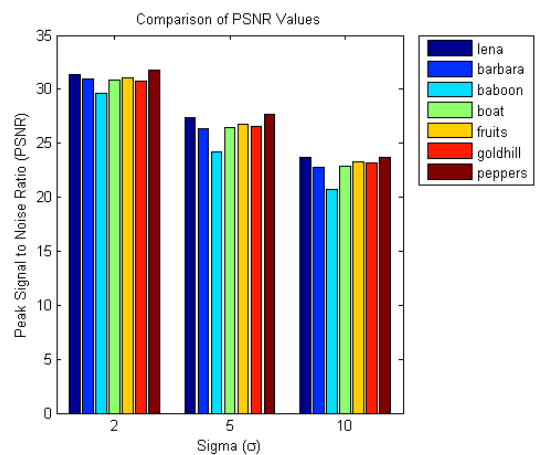


Fig. 16 Comparison among all the images as bar chart

V. CONCLUSION

In this paper, the advantages, applications, and limitations of M-band wavelet transform and its extensions are realized. M-band Wavelet Transforms is a powerful extension to standard DWT. This transform technique is investigated to reduce the major limitations of standard DWT and its extensions in certain signal processing applications.

The history, basic theory, recent trends, and various forms of M-band wavelet transforms with their applications are collectively and comprehensively analysed. Recent developments in M-band wavelet transforms are critically compared with existing forms of WTs. Potential applications are investigated and suggested that can be benefited with the use of different variants of M-band wavelet transforms.

Individual software codes are developed for simulation of selected applications such as Denoising both WTs and M-band wavelet transforms. The performance is statistically validated and compared to determine the advantages and limitations of M-band wavelet transforms over well-established WTs. Promising results are obtained using individual implementation of existing algorithms incorporating novel ideas into well-established frameworks.

ACKNOWLEDGMENT

The authors express their sincere thanks to Prof. Dr. Santi Prasad Maity for his invaluable guidance for this paper.

REFERENCES

- [1] DIGITAL IMAGE PROCESSING – Rafael C. Gonzalez, Richard E. Woods and Steven L. Eddins, Pearson Education.
- [2] The wavelet tutorial by Robi Polikar.
- [3] http://en.wikipedia.org/wiki/Image_noise
- [4] D.L. Donoho, “De-Noising by Soft Thresholding”, *IEEE Trans. Info. Theory* 43, pp. 933-936, 1993.
- [5] S. Grace Chang, Student Member, IEEE, Bin Yu, Senior Member, IEEE, and Martin Vetterli, Fellow, IEEE, “Adaptive Wavelet Thresholding for Image Denoising and Compression”, *IEEE Transactions on Image Processing*, Vol. 9, No. 9, pp. 1532–1546, September 2000.
- [6] Ruban Brar and Rajesh Kumar, “Image Denoising Using Wavelet Thresholding Hybrid Approach”, Proceedings of SARC-IRAJ International Conference, 22nd June 2013, New Delhi, India, ISBN: 978-81-927147-6-9.
- [7] Nima Khademi Kalantari and Pradeep Sen, “Removing the Noise in Monte Carlo Rendering with General Image Denoising Algorithms”, © 2013 The Eurographics Association and Blackwell Publishing Ltd.
- [8] S. M. Mahbubur Rahman, M. Omair Ahmad, Fellow, IEEE, and M. N. S. Swamy, Fellow, IEEE, “Bayesian Wavelet-Based Image Denoising Using the Gauss–Hermite Expansion”, *IEEE Transactions on Image Processing*, Vol. 17, NO. 10, pp. 1755–1770, October 2008.
- [9] Priyanka Kamboj and Versha Rani, “A Brief Study of Various Noise Model and Filtering Techniques”, *Journal of Global Research in Computer Sc.*, Vol 4, No. 4, April 2013.
- [10] D.L. Donoho and I.M. Johnstone, Adapting to unknown smoothness via wavelet shrinkage, *Journal of American Statistical Assoc.*, Vol. 90, no. 432, pp 200-1224, Dec. 1995.
- [11] P.R. Hill, A. Achim, and D.R. Bull, M.E. Al-Mualla, “Image Denoising Using Dual Tree Statistical Models for Complex Wavelet Transform Coefficients Magnitude”, *IEEE Transaction*, 978-1-4799-2341-0/13.
- [12] Tang Hui, Liu Zengli, Chen Lin, Chen Zaiyu, “Wavelet Image Denoising Based on The New Threshold Function”, Proceedings of the 2nd International Conference on Computer Science and Electronics Engineering (ICCSEE 2013).
- [13] Jiecheng Xie, Student Member, IEEE, Dali Zhang, and Wenli Xu, “Spatially Adaptive Wavelet Denoising Using the Minimum Description Length Principle”, *IEEE Transactions on Image Processing*, Vol. 13, NO. 3, pp. 179–187, February 2004.
- [14] Javier Portilla, Vasily Strela, Martin J. Wainwright, Eero P. Simoncelli, “Javier Portilla, Vasily Strela, Martin J. Wainwright, Eero P. Simoncelli”, *IEEE Transactions on Image Processing*, Vol. 12, NO. 11, pp. 1338–1351, November 2003.
- [15] Hari Om, Mantosh Biswas, “An Improved Image Denoising Method Based on Wavelet Thresholding”, *Journal of Signal and Information Processing*, 2012, 3, pp. 109-116, <http://dx.doi.org/10.4236/jsip.2012.31014>.
- [16] Ashish Khare and Uma Shanker Tiwary, Member, IEEE, “A New Method for Deblurring and Denoising of Medical Images using Complex Wavelet Transform”, Proceedings of the 2005 IEEE Engineering in Medicine and Biology 27th Annual Conference, Shanghai, China, September 1-4, 2005.
- [17] Jingyu Yang, Wenli Xu, Yao Wang, and Qionghai Dai, “2-D Anisotropic Dual Tree Complex Wavelet Packets and Its Application to Image Denoising”, *IEEE Transaction*, 978-1-4244-1764-3/08.
- [18] Caroline Chaux, Laurent Duval, Jean-Christophe Pesquet, “Image Analysis Using a Dual-Tree M-Band Wavelet Transform”, *IEEE Transaction on Image Processing*, Volume 15 , Issue 8, pp: 2397 – 2412, August, 2006.
- [19] Chaux, C., Duval, L., Benazza-Benyahia, A., Pesquet, J., “A New Estimator for Image Denoising Using A 2D Dual-tree M-Band Wavelet Decomposition”, *IEEE International Conference on Acoustics, Speech and Signal Processing*, Vol 3, 2006.
- [20] Pravinkumar Rathod, Mrs. A. V. Kulkarni, "Image Resolution Enhancement by Discrete and Stationary Wavelet Decomposition using Bicubic Interpolation", *International Journal of Engineering Research & Technology (IJERT)*, ISSN: 2278-0181, Vol. 2 Issue 11, November – 2013.
- [21] Siddharth Bhalerao, Papiya Dutta, "Image Denoising Using Riesz Wavelet Transform and SVR", *International Journal of Engineering Research & Technology (IJERT)*, ISSN: 2278-0181, Vol. 2 Issue 11, November – 2013.
- [22] Dr. Anna Saro Vijendran, S. Vinod Kumar, "A New Content Based Image Retrieval System by HOG of Wavelet Sub Bands", *International Journal of Engineering Research & Technology (IJERT)*, ISSN: 2278-0181, Vol. 3 Issue 3, March – 2014.
- [23] Arya P Unni, "Satellite Image Enhancement Using 2D Level DWT", *International Journal of Engineering Research & Technology (IJERT)*, ISSN: 2278-0181, Vol. 3 Issue 3, March – 2014.
- [24] J. Tian and R. O. Wells, “A Fast Implementation of Wavelet Transform for M-band Filter Banks”, *Proc. SPIE*, 3391:534-545 (1998).
- [25] Q. Sun, N. Bi, and D. Huang, *An Introduction to Multiband Wavelets*, Zhejiang University Press, China, 2001.